

Global azimuthal seismic anisotropy and the unique plate-motion deformation of Australia

Eric Debayle¹, Brian Kennett² & Keith Priestley³

¹Institut de Physique du Globe de Strasbourg, Ecole et Observatoire des Sciences de la Terre, Centre National de la Recherche Scientifique and Université Louis Pasteur, 61084 Strasbourg, Cedex, France

²Research School of Earth Sciences, The Australian National University, Canberra ACT 0200, Australia

³Bullard Laboratories, University of Cambridge, Cambridge CB3 0EZ, UK

Differences in the thickness of the high-velocity lid underlying continents as imaged by seismic tomography, have fuelled a long debate on the origin of the ‘roots’ of continents^{1–5}. Some of these differences may be reconciled by observations of radial aniso-

tropy between 250 and 300 km depth, with horizontally polarized shear waves travelling faster than vertically polarized ones². This azimuthally averaged anisotropy could arise from present-day deformation at the base of the plate, as has been found for shallower depths beneath ocean basins⁶. Such deformation would also produce significant azimuthal variation, owing to the preferred alignment of highly anisotropic minerals⁷. Here we report global observations of surface-wave azimuthal anisotropy, which indicate that only the continental portion of the Australian plate displays significant azimuthal anisotropy and strong correlation with present-day plate motion in the depth range 175–300 km. Beneath other continents, azimuthal anisotropy is only weakly correlated with plate motion and its depth location is similar to that found beneath oceans. We infer that the fast-moving Australian plate contains the only continental region with a sufficiently large deformation at its base to be transformed into azimuthal anisotropy. Simple shear leading to anisotropy with a plunging axis of symmetry may explain the smaller azimuthal anisotropy beneath other continents.

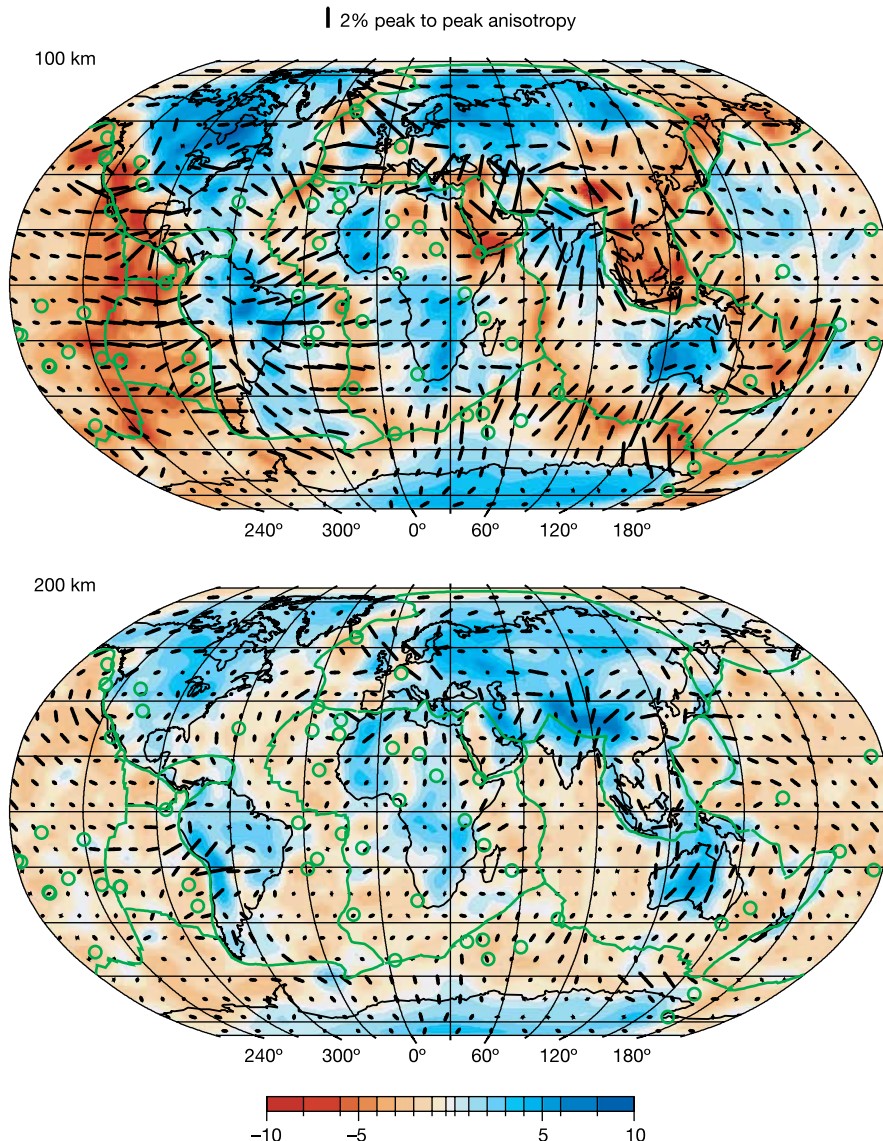


Figure 1 SV-wave heterogeneity and azimuthal anisotropy (black bars oriented along the axis of fast propagation) at 100 and 200 km depth obtained from the inversion of 100,779 Rayleigh waveforms. Hotspot locations are indicated by green circles. The length of the

black bars is proportional to the maximum amplitude of azimuthal anisotropy (bar length for 2% peak to peak anisotropy shown at top). SV-wave perturbations (in per cent relative to PREM) are represented with the colour scale.

Our finding comes in the context of the building of a new surface wave tomographic model of the upper mantle designed to investigate shear wave heterogeneities and azimuthal anisotropy. In the upper mantle, horizontally travelling surface waves provide better vertical resolution than body waves, which are more subject to vertical smearing owing to their steep incidence. The novelty of our approach is to directly extract from surface waves the directions of fast propagation for horizontally travelling ‘SV’ (vertically polarized) waves, with an unprecedented lateral resolution at a global scale, instead of determining anisotropy in group or phase velocity, as in other recent studies^{8,9}. Direct estimates of fast SV directions provide better vertical resolution compared to group or phase velocity measurements, which represent a weighted average of the structure/anisotropy over a frequency-dependent depth interval. Our path coverage (see Supplementary Fig. 1) allows us to resolve anisotropic variations with horizontal wavelengths matching the scale of the lithospheric blocks that have coalesced to form continents (about 1,000–1,500 km). We can therefore better differentiate between different ways of producing anisotropy: the effect of plate motion would be expected to be smooth at continental scale, whereas ancient deformation frozen in the lithosphere displays shorter-scale lateral variations owing to the complex tectonic history of continents.

There is no systematic difference in the depth location of azimuthal anisotropy between continents and oceans, except beneath Australia. Figure 1 shows the azimuthal variations for SV waves superimposed on the pattern of seismic heterogeneities at 100 and 200 km depth in the upper mantle. At 100 km depth, the amplitude of azimuthal anisotropy generally exceeds 2% beneath young oceans, and exhibits highly variable amplitudes beneath continents and old oceanic basins. When old continents are underlain by significant azimuthal anisotropy (as in Australia, India, and North and South America), the anisotropy varies over short horizontal distances. At 200 km depth, the only continent where plate-scale anisotropy is larger than 2% is Australia. Other continents are associated with weak anisotropy, except locally beneath the Tibetan plateau and the Andean subduction zone. Plate-scale anisotropy has also disappeared beneath oceans except beneath the northern Pacific, where weak (<1%) azimuthal anisotropy extends over a broad region.

Figure 2a shows the average amplitude of azimuthal anisotropy as a function of depth in the upper mantle, calculated for Australia, other continents, and oceanic basins. In oceanic regions, the maximum amplitude of azimuthal anisotropy occurs near 100 km depth, in agreement with previous studies that have suggested an intense deformation at the base of oceanic plates^{3,6}. The depth configuration of azimuthal anisotropy beneath Australia in the depth range 150–300 km is similar to that beneath oceans in the depth range 50–200 km but shifted downward by 100 km. Except in the upper 100 km, Australia is completely different from other continents, which display a gentle decrease of anisotropy from 1.4% at 50 km to about 0.6% at 300 km depth.

Further, Australia is the only continental plate where azimuthal anisotropy correlates significantly with present-day plate motion. This peculiar behaviour of the Australian continent is highlighted in the global correlation (Fig. 3) between azimuthal anisotropy and the present-day absolute plate motion (APM). Fast anisotropy directions beneath Australia do not correlate with APM at depths shallower than 150 km, but show strong correlation from 150 km to 300 km depth with a maximum near 200 km. This agrees with previous regional surface wave tomography for the continent^{10–13}. None of the other continents show significant plate-scale correlation between anisotropic directions and APM. The anisotropic signature of the Australian plate is similar to that observed at shallower depths beneath oceans. In young oceanic regions where the lithosphere is expected to be thin, significant correlation

between anisotropy and APM is observed at 50 km depth (Fig. 3) and extends over large regions around the mid-ocean ridges beneath the Pacific, Indian and Atlantic Oceans. At 100 and 150 km depth, the regions where anisotropy correlates with APM shift to the old oceanic basins. This shift suggests that the depth of plate-motion-induced deformation increases with the age of the sea floor and the thickness of the oceanic lithosphere. Figure 2b shows the average correlation between APM and fast anisotropic directions calculated for Australia, other continents, and oceanic basins. The strong correlation between Australian anisotropy and APM is prominent between 150 and 300 km depth. The fast direction beneath the oceans displays, on average, a weaker correlation with APM between 100 and 250 km depth. This weaker correlation between oceanic anisotropy and APM can be related to the observation⁹ that azimuthal anisotropy beneath oceans aligns better with the largest axis of the finite-strain ellipsoid than with the absolute plate motion. Azimuthal anisotropy of continents other than Australia does not correlate at any depth with APM.

Although an accurate prediction of SKS splitting from surface wave azimuthal anisotropy models is not possible (see Methods), we believe that our results provide a qualitative explanation for the

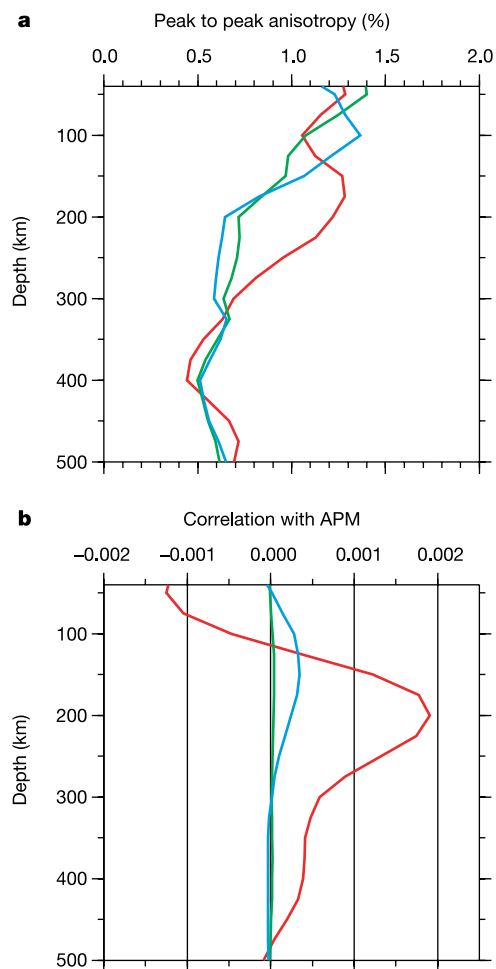


Figure 2 Azimuthal anisotropy amplitude and correlation with plate motion for different tectonic provinces. Green, continents except Australia; red, Australia; and blue, oceans. **a**, Amplitude of peak to peak azimuthal anisotropy as a function of depth. **b**, Correlation between the fast direction of SV waves and absolute plate motion as a function of depth. The correlation coefficient is computed as in Fig. 3, but averaged over the different tectonic provinces.

differences in SKS observations between Australia and the other continents¹⁴. SKS studies generally show typical delay times close to 1 s in most continental regions¹⁵, but only null¹⁶ or very weak¹⁷ splitting beneath Australia. A vertically travelling wave passing through two anisotropic layers with orthogonal directions as found beneath Australia (Fig. 1) would undergo a null or very weak splitting if each layer produced a similar time separation between the fast and slow polarized S-waves. Beneath other continents, weak influence of basal drag on the lithosphere may explain why azimuthal anisotropy is observed only in a layer located in the uppermost 100 km of the mantle. The complex organization of surface wave azimuthal anisotropy present within this layer, and the good agreement between SKS fast directions and fossil geological trends generally observed for continents other than Australia, form the basis for attributing this shallow anisotropic layer (whose thickness is compatible with typical observed SKS delay times) to deformation frozen in the lithosphere. The similar depth behaviour and complex organization of anisotropy down to about 150 km depth observed beneath Australia and other continents (Figs 1 and 2a) suggests that frozen deformation in the lithosphere is also the explanation of shallow upper mantle azimuthal anisotropy beneath Australia.

Laboratory experiments on olivine aggregates suggest that simple shear at the base of a moving plate will produce anisotropy in olivine with a fast *a* axis that follows the principal extension direction for modestly deformed aggregates and aligns with the direction of flow for large deformation¹⁸. Complications occur under water-rich conditions¹⁹ that are not common in the upper mantle²⁰ and are probably confined to subduction zones or regions where upwelling material contains a large amount of water¹⁹. For relatively water-poor olivine, modest simple shear should therefore produce anisotropy with a plunging *a* axis. For surface waves, although the azimuthal variation of Rayleigh wave velocity gradually reduces when the *a* axis departs from the horizontal, the direction of the fastest Rayleigh waves remains in the vertical plane containing the *a*

axis²¹. Our results therefore suggest that the Australian plate is the only continental plate whose motion is fast enough to produce large scale deformation at its base. The slower horizontal motion of other continental plates may produce smaller basal deformation, and thus a larger proportion of olivine crystals with a plunging axis of symmetry and a weaker azimuthal anisotropy. At depths greater than 220 km, enrichment in clinopyroxene may also contribute to the vanishing of anisotropy²².

This basal drag mechanism can explain both the radial and the azimuthal anisotropy of the Australian continent. If the lattice-preferred orientation of olivine crystals is the main mechanism responsible for upper mantle anisotropy⁷, the existence of significant azimuthal anisotropy with coherent directions over broad regions beneath Australia implies that radial anisotropy with SH (horizontally polarized) waves faster than SV waves should also be present to the same depth¹². Radial anisotropy with SH velocities greater than SV velocities ('SH > SV') has indeed been observed beneath Australia down to at least 250 km depth in previous regional^{12,23} and global studies².

Weak azimuthal anisotropy as observed under other continents is compatible with a modest SH > SV radial anisotropy depending on the dip and proportion of oriented olivine crystals. However, the large SH > SV radial anisotropy observed at the base of continents from 250 to 400 km depth by Gung *et al.*² is hard to reconcile with our observation of small azimuthal anisotropy and with the typical 1 s delay time in SKS studies. This incompatibility provides a global scale illustration of the problem of explaining the amplitude of surface wave radial anisotropy with current petrological models, a well-documented problem in regional studies^{3,12,24}. To achieve large SH > SV radial anisotropy with weak azimuthal anisotropy, the olivine crystals need to be preferentially aligned in the horizontal plane, but randomly oriented. Small scale convection due to irregularities of the base of the high-velocity lid or perturbations by mantle plumes can produce such effects.

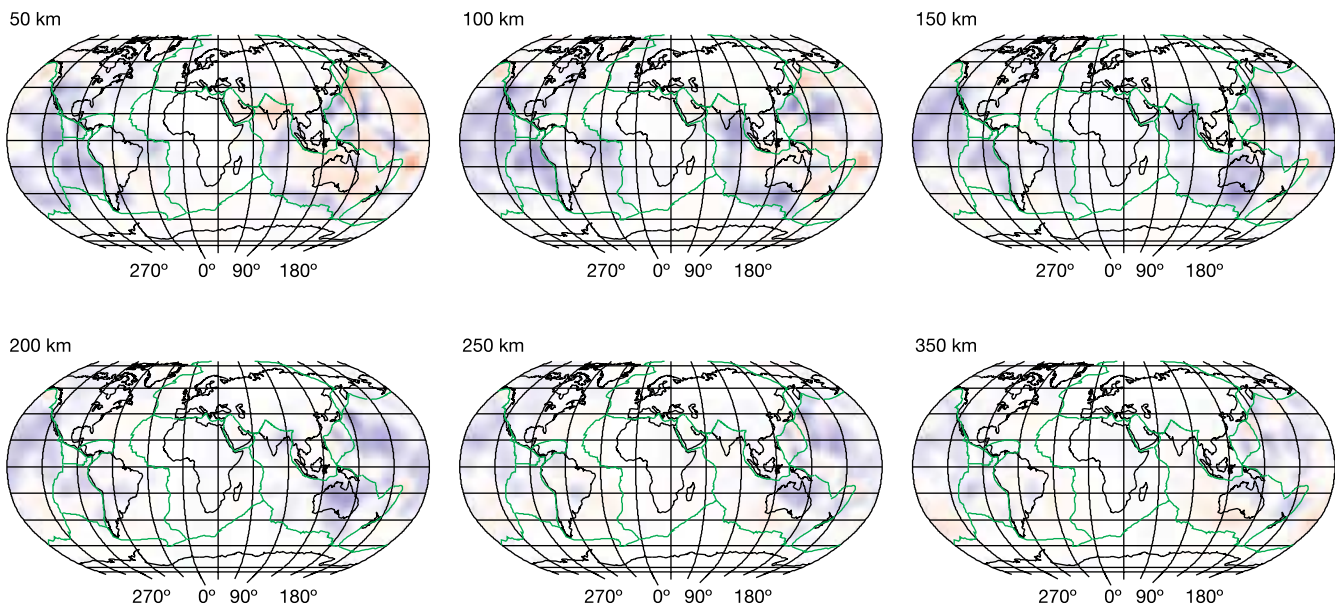


Figure 3 Correlation between fast direction of SV waves and plate motion directions. APM is derived from model Nuvel-1³¹ by imposing a null average rotation of the lithosphere. The correlation coefficient is defined as $|\text{FastSV}||\text{APM}| \cos[2(\phi)]$, where *FastSV* is the fast SV wave vector, *APM* is the absolute plate motion vector and ϕ is the angle between the two vectors. Good correlation (parallelism of the two vectors) is represented in blue, weak correlation is represented in white and bad correlation

(orthogonality) is represented in red. The colour scales are symmetric, adapted to cover the full range of values at each depth (shown at top left of each panel). The amplitude of the correlation coefficient is not shown, as it depends on the strength of anisotropy and is difficult to interpret. Plate boundaries are indicated with green lines.

Our model provides an explanation for SKS observations in continental regions, on the simple basis that anisotropy due to plate motion differs between continental plates. Additional data will be needed to investigate in more detail the global pattern of radial anisotropy in seismic parameters and to reconcile it with other anisotropic observations. Although seismic anisotropy provides a unique way to investigate deformation of the upper mantle, it is increasingly clear that the assumptions underlying anisotropic observations must continue to be questioned. □

Methods

Our model is an 'SV' model constrained by fundamental and higher mode Rayleigh waves (as in ref. 4), but we include azimuthal anisotropy in the inversion and include many short epicentre–station paths (see Supplementary Fig. 2) to improve the lateral resolution of upper mantle structure²⁵. The data set consists of 100,779 Rayleigh waveforms that provide a dense global coverage (see Supplementary Fig. 1), although variations due to the uneven distribution of events and station are inevitable. The number of crossing rays per cell (400 × 400 km) varies between 20 and 2,800 for continents, ensuring redundancy in the data even where ray coverage is the poorest (Africa and Antarctica).

Model construction

Our model is built using a two step tomographic procedure²⁵. First, an automated nonlinear waveform inversion technique^{10,26} is used to model each individual Rayleigh waveform in terms of a depth-dependent SV-wave velocity model representing the average mantle structure along the path. The one-dimensional path-average models are then combined in a tomographic inversion²⁵ to retrieve simultaneously the three-dimensional SV-wave velocity structure and the azimuthal anisotropy of SV waves. The procedure exploits the azimuthal dependence of the Rayleigh wave phase and group velocities in a slightly anisotropic medium²⁷. This azimuthal dependence contains terms in $\cos(2\theta)$, $\sin(2\theta)$ and $\cos(4\theta)$, $\sin(4\theta)$, where θ is the azimuth relative to north, and has been recently inverted to retrieve the global azimuthal variations in the group or phase velocities at different periods^{8,9}. The azimuthal terms can also be inverted in depth, as they depend on several combinations of the elastic parameters via a set of partial derivatives proportional to the partial derivatives of a transversely isotropic medium with a vertical axis of symmetry²⁸. The combinations of elastic parameters best resolved by Rayleigh waves involve at each depth an isotropic term that corresponds to the SV-wave velocity and two azimuthal terms that display a variation in $\cos(2\theta)$, $\sin(2\theta)$ relative to the direction of maximum velocity. In a long period approximation, the one-dimensional SV-wave velocity models obtained after the waveform fitting depend on these three combinations of elastic parameters, which control the velocities of SV waves propagating horizontally for azimuth θ (ref. 29). For an olivine model, the direction of maximum velocity coincides with the horizontal projection of the fast a axis of olivine crystals. Both the non-azimuthal term and the direction of fast seismic velocities extracted from the $\cos(2\theta)$, $\sin(2\theta)$ azimuthal terms are represented on Fig. 1.

Resolution issues and model tests

A Voronoi diagram built using the approach of ref. 25 (see Supplementary Fig. 3) provides a useful guide to our ability to resolve azimuthal anisotropy with our data coverage. The cells in Supplementary Fig. 3 are the smallest for which the local distribution of rays ensures that the $\cos(2\theta)$, $\sin(2\theta)$ SV-wave azimuthal variation can be resolved. This 'optimized Voronoi' diagram is based on the ray distribution alone and does not incorporate any *a priori* information on the data or the model, nor does it take into account the influence of different parameter choices. However, it provides a useful proxy for resolution when combined with the horizontal degree of smoothing imposed *a priori* on the tomographic inversion. We impose lateral smoothness through a gaussian correlation function with a standard deviation of 400 km, chosen to minimize the trade-off between isotropic and anisotropic parameters. Azimuthal anisotropy is guaranteed to be resolved when the size of the Voronoi cells in Supplementary Fig. 3 is smaller than, or comparable to, a circular surface with a minimum diameter of about 1,000 km. Azimuthal anisotropy resolution is achieved for 1,000-km circular regions beneath most continents and at the Voronoi level for western Africa and Antarctica.

We have performed a variety of tests using real and synthetic data to estimate potential leakage by non-inverted parameters, vertical resolution and how well our model can predict SKS observations. We have found (1) that contamination by non-inverted parameters, such as the 4θ azimuthal variation of the Rayleigh waves phase velocity or the B and H combinations of elastic coefficients as defined in ref. 28, is weak (Supplementary Fig. 4), (2) that our vertical resolution is sufficient to recover a change in anisotropic direction at the bottom of continental plates (Supplementary Fig. 5), and (3) that it is not possible to make accurate predictions of SKS observations from our tomographic model. In fact, the length scales over which SKS results vary in continental regions are often below the horizontal resolution of surface waves. Furthermore, vertical smearing (Supplementary Fig. 5) can bias the splitting prediction (Supplementary Fig. 6b), and the SKS predictions themselves (Supplementary Fig. 6c) rely on a theory³⁰ that does not properly handle inclined symmetry axes and is only effective for rather long period waves.

Received 2 July; accepted 29 November 2004; doi:10.1038/nature03247.

1. Jordan, T. H. The continental tectosphere. *Rev. Geophys.* **13**, 1–12 (1975).

- Gung, Y., Panning, M. & Romanowicz, B. Global anisotropy and the thickness of continents. *Nature* **422**, 707–711 (2003).
- Ekström, G. & Dziewonski, A. M. The unique anisotropy of the Pacific upper mantle. *Nature* **394**, 168–172 (1998).
- Ritsema, J., van Heijst, H. J. & Woodhouse, J. H. Global transition zone tomography. *J. Geophys. Res.* **109**, B02302, doi:10.1029/2003JB002610 (2004).
- Montagner, J. P. & Tanimoto, T. Global upper mantle tomography of seismic velocities and anisotropies. *J. Geophys. Res.* **96**, 20337–20351 (1991).
- Forsyth, D. W. The early structural evolution and anisotropy of the oceanic upper mantle. *Geophys. J. R. Astron. Soc.* **43**, 103–162 (1975).
- Nicolas, A. & Christensen, N. I. in *Composition, Structure and Dynamics of the Lithosphere-Asthenosphere System* (eds Fuchs, F. & Froidevaux, C.) 111–123 (Geodyn. Ser. Vol. 16, AGU, Washington DC, 1987).
- Trampert, J. & Woodhouse, J. H. Global anisotropic phase velocity maps for the fundamental mode surface waves between 40 and 150 s. *Geophys. J. Int.* **154**, 154–165 (2003).
- Becker, T. W., Kellogg, J. B., Ekstrom, G. & O'Connell, R. J. Comparison of azimuthal seismic anisotropy from surface waves and finite strain from global mantle-circulation models. *Geophys. J. Int.* **155**, 696–714 (2003).
- Debayle, E. SV-wave azimuthal anisotropy in the Australian upper-mantle: Preliminary results from automated Rayleigh waveform inversion. *Geophys. J. Int.* **137**, 747–754 (1999).
- Debayle, E. & Kennett, B. L. N. The Australian continental upper mantle: structure and deformation inferred from surface waves. *J. Geophys. Res.* **105**, 25423–25450 (2000).
- Debayle, E. & Kennett, B. L. N. Anisotropy in the Australasian upper mantle from Love and Rayleigh waveform inversion. *Earth Planet. Sci. Lett.* **184**, 339–351 (2000).
- Simons, F. J. & van der Hilst, R. D. Seismic and mechanical anisotropy and the past and present deformation of the Australian lithosphere. *Earth Planet. Sci. Lett.* **211**, 271–286 (2003).
- Park, J. & Levin, V. Seismic anisotropy: Tracing plate dynamics in the mantle. *Science* **296**, 485–489 (2002).
- Savage, M. K. Seismic anisotropy and mantle deformation: What have we learned from shear wave splitting? *Rev. Geophys.* **37**, 65–106 (1999).
- Ozalabey, S. & Chen, W. P. Frequency dependent analysis of SKS/SKKS waveforms observed in Australia: evidence for null birefringence. *Phys. Earth Planet. Inter.* **114**, 197–210 (1999).
- Clitheroe, G. & van der Hilst, R. D. in *Structure and Evolution of the Australian Continent* (eds Braun, J., Dooley, J., Goleby, B., van der Hilst, R. & Klootwijk, C.) 73–78 (Geodyn. Monogr. 26, AGU, Washington DC, 1998).
- Zhang, S. & Karato, S. I. Lattice preferred orientation of olivine aggregate deformed in simple shear. *Nature* **375**, 774–777 (1995).
- Jung, H. & Karato, S. I. Water-induced fabric transitions in olivine. *Science* **293**, 1460–1463 (2001).
- Kaminski, E. The influence of water on the development of lattice preferred orientation in olivine aggregates. *Geophys. Res. Lett.* **29**, 12, doi:10.1029/2002GL014710 (2002).
- Babuska, V. & Cara, M. *Seismic Anisotropy in the Earth* (Kluwer Academic, Dordrecht, 1991).
- Beghein, C. & Trampert, J. Probability density functions for radial anisotropy: implications for the upper 1200 km of the mantle. *Earth Planet. Sci. Lett.* **217**, 151–162 (2003).
- Gaherty, J. B. & Jordan, T. Lehmann discontinuity as the base of an anisotropic layer beneath continents. *Science* **268**, 1468–1471 (1995).
- Maupin, V. & Cara, M. Love-Rayleigh wave incompatibility and possible deep upper mantle anisotropy in the Iberian peninsula. *Pure Appl. Geophys.* **138**, 429–444 (1992).
- Debayle, E. & Sambridge, M. Inversion of massive surface wave data sets: Model construction and resolution assessment. *J. Geophys. Res.* **109**, B02316 doi:10.1029/2003JB002652, (2004).
- Cara, M. & Lévêque, J. J. Waveform inversion using secondary observables. *Geophys. Res. Lett.* **14**, 1046–1049 (1987).
- Smith, M. & Dahlen, F. The azimuthal dependence of Love and Rayleigh wave propagation in a slightly anisotropic medium. *J. Geophys. Res.* **78**, 3321–3333 (1973).
- Montagner, J. P. & Nataf, H. C. A simple method for inverting the azimuthal anisotropy of surface waves. *J. Geophys. Res.* **91**, 511–520 (1986).
- Lévêque, J. J., Debayle, E. & Maupin, V. Anisotropy in the Indian Ocean upper mantle from Rayleigh- and Love-waveform inversion. *Geophys. J. Int.* **133**, 529–540 (1998).
- Montagner, J. P., Griot-Pommere, D. A. & Lavé, J. How to relate body wave and surface wave anisotropy? *J. Geophys. Res.* **105** (B8), 19015–19027 (2000).
- DeMets, C., Gordon, R. G., Argus, D. F. & Stein, S. Current plate motion. *Geophys. J. Int.* **101**, 425–478 (1990).

Supplementary Information accompanies the paper on www.nature.com/nature.

Acknowledgements This work was supported by programme DyETI conducted by the French Institut National des Sciences de l'Univers (INSU). The data used in this work were obtained from the GEOSCOPE, GDSN, IDA, MEDNET and GTSN permanent seismograph networks, and completed with data collected after the PASSCAL broadband experiments, the SKIPPY and subsequent broadband deployments in Australia, and the INSU deployments in the Horn of Africa and the Pacific (PLUME experiment). Supercomputer facilities were provided by the IDRIS and CINES national centres in France. Special thanks to J. M. Brendle at EOST for technical support, S. Fishwick for providing broadband data from the Western Australian craton field deployment, the staff of the Research School of Earth Science who collected the SKIPPY data in the field, and A. Maggi for suggestions that improved the manuscript.

Competing interests statement The authors declare that they have no competing financial interests.

Correspondence and requests for materials should be addressed to E.D. (Eric.Debayle@eost.u-strasbg.fr).